

## Electronic bands structure and gap in mid-infrared detector InAs/GaSb type II nanostructure superlattice

A. Boutramine, A. Nafidi, D. Barkissy, A. Hannour, M. Massaq, H. Chaib

Laboratory of Condensed Matter Physics and Nanomaterials for Renewable Energy University Ibn Zohr, 80000 Agadir, Morocco.

### ABSTRACT

We present here theoretical study of the electronic bands structure  $E(k)$  of InAs ( $d_1=25 \text{ \AA}$ )/GaSb ( $d_2=25 \text{ \AA}$ ) type II superlattice at 4.2 K performed in the envelope function formalism. We study the effect of  $d_1$  and the offset  $\Lambda$ , between heavy holes bands edges of InAs and GaSb, on the band gap  $E_g(\Gamma)$ , at the center  $\Gamma$  of the first Brillouin zone, and the semiconductor-to-semimetal transition.  $E_g(\Gamma, T)$  decreases from 288.7 meV at 4.2 K to 230 meV at 300K. In the investigated temperature range, the cut-off wavelength  $4.3 \mu\text{m} \leq \lambda_c \leq 5.4 \mu\text{m}$  situates this sample as mid-wavelength infrared detector (MWIR). Our results are in good agreement with the experimental data realized by C. Cervera et al.

**Keywords** - Bands structure, envelope function formalism, InAs/GaSb type II superlattice, mid-infrared detector, semiconductor-semimetal transition.

### I. INTRODUCTION

The idea of the type II InAs/GaSb superlattice (T2SL) was firstly suggested by Sai-Halasz and coworkers in 1977 [1]. The application of such (SL), only after several years, was proposed as an infrared sensing material by Smith and Mailhoit in 1987 [2]. Since then, the (T2SL) have made significant progress and attracted increasing interest for mid (3–5 $\mu\text{m}$ ) [3] and long wavelength infrared region (8–12 $\mu\text{m}$ ) [4].

This system characterized by the type II alignment wherein the bottom of the conduction band of InAs lies well below the top of the valence band of GaSb [1-5] (see Fig.1). It has been established that the overlap between these two bands is in the vicinity of 150 meV [2-3]. This structure leads to the separation of electrons and holes into the InAs and GaSb layers, respectively. This peculiar relationship of band edge separation creates a situation in which the fundamental band gap energy of this superlattice can be tailored by varying the thickness of the constituents InAs and GaSb layers, and switch from being positive to negative. It follows that a wide range of operation wavelengths can be covered, and the system undergoes a semiconductor to semimetal transition that is expected to occur when the InAs conduction band is lower in energy than the GaSb valence band [6].

In order to study the electronic bands structure of InAs/GaSb, intensive theoretical investigations have been developed. The most widely used are the empirical tight binding method [7] and the k.p model [8] including the envelope-function formalism [9].

In this paper we report the bands structure and the effect of  $d_1$ , the offset  $\Lambda$ , the temperature on the band gap  $E_g(\Gamma)$  and the semiconductor-to-semimetal transition.

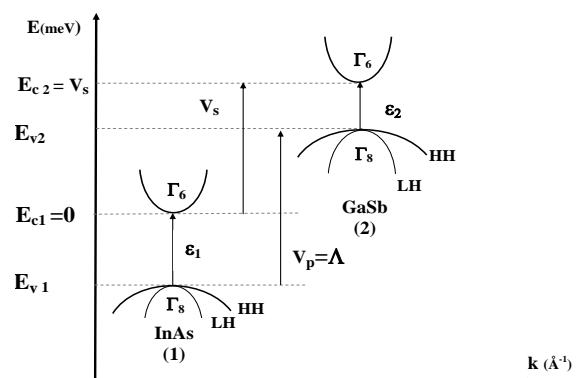


**Fig. 1:** Schematic illustration of the energy band alignment of InAs/GaSb.  $E_{c1}$  (resp.  $E_{c2}$ ) and  $E_{v1}$  (resp.  $E_{v2}$ ) are the conduction and valence band of InAs (resp. GaSb). The LH and HH indices refer to light holes and heavy holes, respectively.  $V_s$  and  $V_p$  are the conduction and valence band offsets which play the roles as the barriers for confining electrons and holes, respectively.

### II. THEORY OF ELECTRONIC BANDS STRUCTURE

Calculations of the spectra of energy were performed in the envelope function formalism. We will show that this technique can be used with a small number of experimental bands structure parameters. The origin of energy is taken at the bottom  $\Gamma_6$  of InAs conduction band (Fig.1).

#### 2.1. Light particle subbands

Applying the Bloch theorem and the use of

appropriate matching conditions at the interface, leads to the general dispersion relation of the (SL)

$$\cos(k_z d) = \cos(k_1 d_1) \cos(k_2 d_2) - \frac{1}{2} \left[ \left( \xi + \frac{1}{\xi} \right) + \frac{k_p^2}{4k_1 k_2} \left( r + \frac{1}{r} - 2 \right) \right] \sin(k_1 d_1) \sin(k_2 d_2) \quad (1)$$

Here,  $k_1$  and  $k_2$  are the wave vectors along the z axis. The two-dimensional wave Vector  $k_p(k_x, k_y)$  describes the motion of particles perpendicularly to  $k_z$ .  $d_1$  and  $d_2$  refer to the thickness of InAs and GaSb layers, respectively. Finally  $\xi$  is given by:

$$\xi = \frac{k_1}{k_2} r = \frac{k_1}{k_2} \frac{E - \varepsilon_2 - \Lambda}{E - \varepsilon_2} \quad (2)$$

At given energy, the two-band Kane model [10] gives the wave vector ( $k_1^2 + k_p^2$ ) in each host material by:

$$\begin{aligned} \frac{2}{3} P^2 h^2 (k_1^2 + k_p^2) &= (E - \varepsilon_1) E && \text{:InAs} \\ \frac{2}{3} P^2 h^2 (k_2^2 + k_p^2) &= (E - \varepsilon_2 - \Lambda)(E - \Lambda) && \text{:GaSb} \end{aligned} \quad (3)$$

$\varepsilon_1$  and  $\varepsilon_2$  are the interaction band gaps of InAs and GaSb, respectively. We use the valence band offset  $\Lambda = 570$  meV determined by far-infrared absorption in a magnetic field for different hydrostatic pressures [11].  $P$  is the Kane matrix element which is taken to be  $1.36 \cdot 10^6$  J/kg for InAs and  $1.41 \cdot 10^6$  J/kg for GaSb [12]. At given energy  $E$ , a (SL) state of wave vector  $k_z$  exists if the right-hand-side of (1) lies in the range  $(-1, +1)$  that implies  $-\pi/d \leq k_z \leq \pi/d$  in the first Brillouin zone.

### 2.2. Heavy hole subbands

The (SL) heavy hole subbands are obtained from the same equation (1) with:

$$\begin{aligned} k_1^2 + k_p^2 &= \frac{2m_{HH}^*}{h^2} (E - \Lambda) && \text{:InAs} \\ k_2^2 + k_p^2 &= \frac{2m_{HH}^*}{h^2} E && \text{:GaSb} \end{aligned} \quad (4)$$

$$\xi = \frac{k_1}{k_2} r = \frac{k_1 m_{HH}^*}{k_2 m_{HH}^*} \quad (5)$$

Where  $m_{1HH}^* = 0.41m_0$  and  $m_{2HH}^* = 0.44m_0$  are the heavy hole masses in InAs and GaSb, respectively. These experimental values are determined respectively by F. Matossi et al in p-type InAs [13], and A. Filion by magneto-photoconductivity in GaSb at 4.2 K [14].

## III. RESULTS AND DISCUSSIONS

When  $d_1$  increase, Fig.2 shows that the energy of electrons  $E_1$ , in the InAs layer, decreases. While the energy of heavy holes  $HH_1$ , in GaSb, increases in agreement with the prevision of [15]. The crossover of  $E_1$  and  $HH_1$  occurs when  $d_1$ (InAs) reaches a critical value  $d_{1c} = 74 \text{ \AA}$ , corresponding to the energy

light particle (electron and light hole) subbands given by the expression [9]:

$E_c = 558$  meV. Then, the (T2SL) achieves a semiconductor-to-semimetal transition. After,  $E_1$  lie down  $HH_1$  and  $E_g(\Gamma)$  becomes negative assuming a semimetallic conductivity. In this case, the electrons flood from the GaSb valence band to the InAs conduction band minimum.

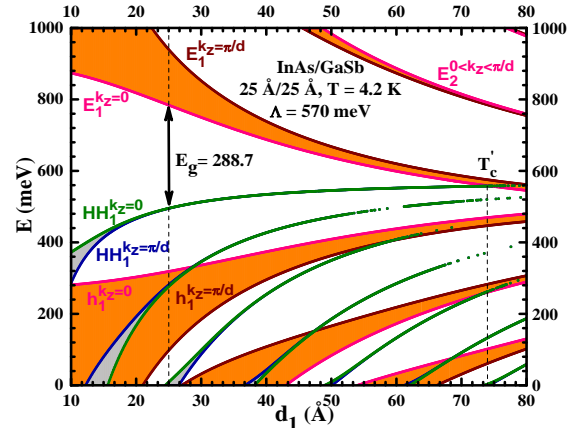


Fig. 2: Energy position and width of the conduction ( $E_1$ ), heavy-hole ( $HH_1$ ), and light-hole ( $h_1$ ) subbands calculated at 4.2 K, in the first Brillouin zone, as a function of the  $d_1$ (InAs) layer thickness.

In the Fig.3, when the offset  $\Lambda$  increases, the band gap  $E_g(\Gamma)$  increases to a maximum near 600 meV at  $\Lambda = 44$  meV. After it decreases to zero at the transition semiconductor-to-semimetal conductivity, and becomes negative accusing a semimetallic conduction after  $\Lambda_c = 990$  meV at  $T = 4.2$  K. Our chosen value of 570 meV is indicated by a vertical dashed line. This offset is closed to 500 meV used

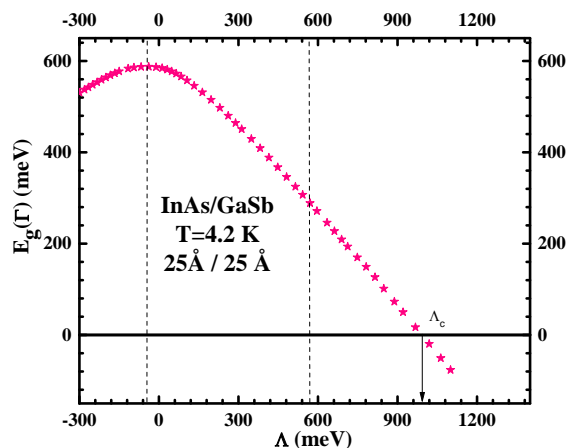
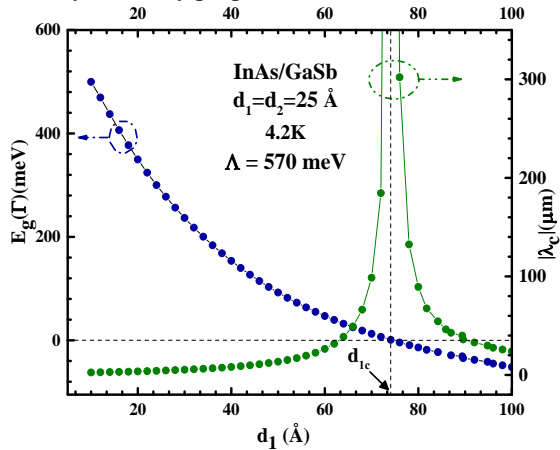


Fig. 3: The band gap  $E_g(\Gamma)$  at  $\Gamma$ , as function the offset  $\Lambda$  at 4.2 K, for the investigated InAs/GaSb (SL) with  $d_1 = d_2 = 25 \text{ \AA}$ .

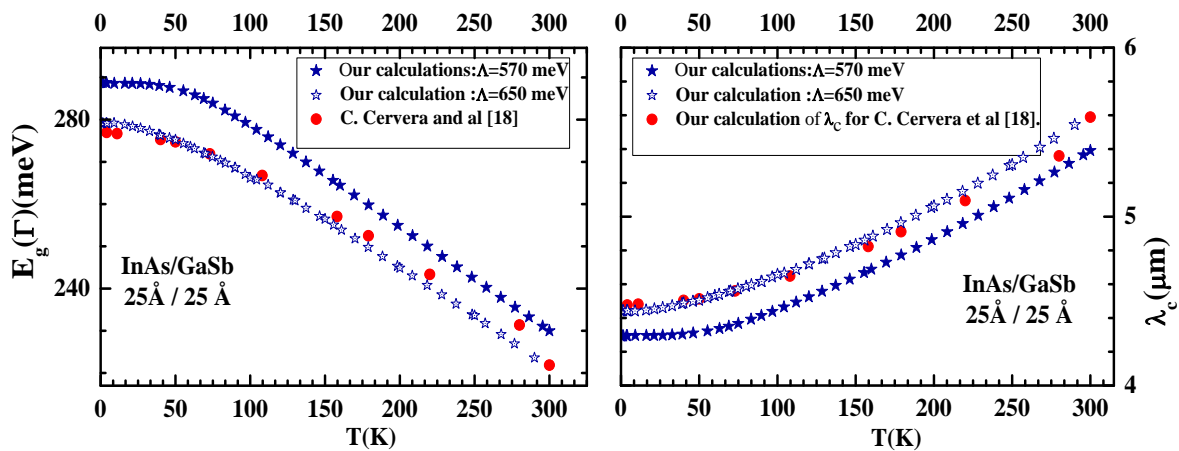
by L. L. Li et al [15] for a sample with  $d_1 = 23.5 \text{ \AA}$  and  $d_2 = 24 \text{ \AA}$ .

Fig.4 shows that when  $d_1$  increases  $E_g(\Gamma)$  decreases, go to zero at the transition point  $T'_c$ , and becomes negative with a semimetal conductivity. The cut-off wavelength  $|\lambda_c|$  diverge at  $T'_c$  with  $d_{1c}=74 \text{ \AA}$ . This band gap variation can be understood using this simple model; the InAs layer acts as a quantum well confining the conduction electrons. It's well known that the energy level of a particle is closely inversely proportional to its effective mass



**Fig.4:** Band gap energy  $E_g(\Gamma)$  and the cut-off wavelength  $|\lambda_c|$  as a function of InAs layer width  $d_1$  at 4.2K.

and the square of the well width. When the InAs well width increases, the energy level of the electrons miniband in the InAs layer decreases, leading to a decrease in the band gap. On another hand, the GaSb layer is envisioned as a well for holes. Because of the bigger GaSb valence band effective mass, the dependence of the energy on the well width becomes much smaller. This behavior can also be explained by the “model-solid theory” of Van de Walle and Martin [16], which describes the shift in position of the conduction and valence band when the volume of the crystal changes (id  $d_1$  and/or  $d_2$ ).



**Fig.5:** Temperature dependence of the band gap  $E_g$  (Left panel). The right panel shows the Cut-off wavelength  $\lambda_c$ , at the center  $\Gamma$ -point of the first Brillion zone.

Significant research and number of empirical models has been developed to describe the temperature-dependent behavior of band gap on various semiconductors. Among them, the Varshni model [17] suggests that in semiconductors the temperature dependence of band gap derives partly from the lattice expansion of the crystal and partly from the electron-phonon interaction.

Using the value of  $\epsilon_1$  and  $\epsilon_2$  at different temperatures between 4.2 K and 300 K, we get the temperature dependence of the band gap  $E_g(\Gamma)$  in Fig.5 which can be described quite well by the empirical Varshni form [17].

$$E_g(T) = E_g(T=0) - \alpha \frac{T^2}{T + \beta} \text{ (meV)} \quad (6)$$

The zero temperature extrapolated energy gap  $E_g(T=0)$ , and the coefficients  $\alpha$  and  $\beta$  for our (SL) are listed in Tab.1.

	$E_g(0)$ (meV)	$\alpha$ (meV/K)	$\beta$ (K)
InAs/GaSb <sup>[18]</sup>	277	0.34	254
InAs/GaSb ( $\Lambda=570$ meV)	288.8	0,36	241
InAs/GaSb ( $\Lambda=650$ meV)	279.2	0.37	258

**Tab.1:** Fit parameters for temperature dependence of superlattice band gap.

The both experimental results and our calculated band-gap (and the cut-off wavelength) as function of temperature are shown in Fig.5. This shift of band gap arises mainly from the decreasing of the potential seen by the electrons in the material due to the increase of the interatomic spacing. The detection cut-off wavelength was calculated

using the expression:

$$\lambda_c(\mu\text{m}) = \frac{1240}{E_g(\text{meV})} \quad (7)$$

We note that the offset  $\Lambda$  of the sample characterized by Cervera et al. is not indicated in [18]. According to our calculations the offset  $\Lambda=650$  meV give a good agreement of our calculations with the experimental data in [18]. For  $\Lambda=570$  meV, the fundamental gap energy decreases from 288.7 meV at 4.2 K to 230 meV at 300K. In the investigated temperature range, the cut-off wavelength  $4.3\mu\text{m} \leq \lambda_c \leq 5.4\mu\text{m}$  situates this sample as a mid-infrared detector (MWIR).

#### IV. CONCLUSION

Our calculations of the electronic bands structure  $E(d_1)$  at 4.2K had shown that when  $d_1$  and the offset  $\Lambda$  increases,  $E_g$  decreases to zero with a transition semiconductor to semimetal, respectively, for  $d_{1c}=74 \text{ \AA}$  and  $\Lambda_c =990$  meV. When the temperature increases, the  $E_g(\Gamma, T)$  decreases from 288.7 meV at 4.2 K to 230 meV at 300K corresponding to the cut-off wavelength  $4.3\mu\text{m} \leq \lambda_c \leq 5.4\mu\text{m}$  which situates this sample as mid-wavelength infrared detector (MWIR). Our results are in good agreement with the experimental data realized by C.Cervera, et al. for an offset  $\Lambda =650$  meV. Note that we had observed a semiconductor type n conduction mechanism in a narrow gap, two-dimensional and far-infrared detector HgTe/CdTe type III superlattice [19].

#### REFERENCES

- [1] G. A. Sai-Halasz, R. Tsu, and L. Esak, A new semiconductor superlattice *Appl. Phys. Lett.* 30, 1977, 651-653.
- [2] D. L. Smith and C. Mailhot, Proposal for strained type II superlattice, *infrared detectors, J.Appl.Phys.*62, 1987, 2545-2548.
- [3] A. Rogalski, Material considerations for third generation infrared photon detectors, *Infrared Phys.Technol.* 50, 2007, 240-252.
- [4] H. Mohseni, M. Razeghi, Long-Wavelength Type-II Photodiodes operating at room temperature, *IEEE Photon. Technol. Lett.* 13, 2001, 517-519.
- [5] G. A. Sai-Halasz, L.L.Chang, J.M.Walter, C.A. Chang, and L. Esaki, Optical absorption of  $\text{In}_{1-x}\text{Ga}_x\text{As-GaSb}_{1-y}\text{As}_y$  superlattices, *Solide State Commun.* 27, 1978, 935-939.
- [6] M. Altarelli, Electronic structure and semiconductor-semimetal transition in InAs-Gasb superlattices , *Phys. Rev. B* 28, 1983, 842-845.
- [7] Wei Y and M.Razeghi, Modeling Type II InAs/GaSb superlattices using empirical tight-binding method: new aspects, *Proc. of SPIE Vol. 5359*, 2004, 301-308.
- [8] Mohseni H, Lit vinov V I and M. Razeghi, Interface-induced suppression of the Auger recombination in type-II InAs/GaSb superlattices, *Phys. Rev.B*, 58, 1998,15378-15380.
- [9] G. Bastard, Superlattice band structure in the envelope-function approximation, *Phys.Rev. B*, Vol 24, 1981, 5693-5697; A. Nafidi, et al, in *Book of Abstracts of the International Conference on Theoretical Physics (HT 2002)*, Paris, France, 22–27 July 2002, 274–275.
- [10] E.O. Kane, Band structure of indium antimonid, *J. Phys. Chem. Solids* 1(4), 1957 ,249–261.
- [11] L. M. Claessen,J. C. Maan, M. Altarelli, and P. Wyder, Pressure Dependence of Band Offsets in an InAs-GaSb Superlattice, *Appl. Phys. Lett.* 57, 1986, 2556-2559.
- [12] Jérôme faist, Quantum cascade lasers, *1st edn. ISBN 978-0-19-852824-1 (Oxford university press)*, 2013, p. 28
- [13] F. Matossi and F. Stern, Temperature Dependence of Optical Absorption in p-Type Indium Arsenide, *Phys.Rev. B*, Vol 111, 1958, 472-475.
- [14] Filion and E. Fortin, Photoconductivity associated with landau structure in GaSb, *Phys. Rev. B* 8, 1973, 3852-3860.
- [15] L. L. Li,1 W. Xu, J. Zhang, and Y. L. Shi , Midinfrared absorption by InAs/GaSb type-II superlattices, *J. Appl. Phys.* 105, 2009, 013115.
- [16] C. G. Van de Walle, Band lineups and deformation potentials in the model-solid theory, *Phys. Rev. B* 39, 1989.
- [17] Y.P.Varshni, Temperature dependence of the energy gap in semiconductors, *Physica* 34, 1967, 149-154.
- [18] C. Cervera, J. B. Rodriguez, J. P. Perez, H. Ait-Kaci, R. Chaghi, L. Konczewicz, S. Contreras, and P. Christol, Unambiguous determination of carrier concentration and mobility for InAs/GaSb superlattice photodiode optimization, *J. Appl. Phys.*106, 2009, 033709.
- [19] M. Braigue, A. Nafidi, et al, Correlation Between Band Structure and Magneto-Transport Properties in HgTe/CdTe Two Dimensional Far-Infrared Detector Superlattice, *Journal of Low Temperature Physics, Volume 171, Issue 5-6, Springer*, 2013,808-8.